International Journal of Power Electronics and Drive System (IJPEDS)
Vol. 12, No. 2, June 2021, pp. 1265~1274
ISSN: 2088-8694, DOI: 10.11591/ijpeds.v12.i2.pp1265-1274

Analysis and design of class E-LCCL compensation circuit topology circuit topology for capacitive power transfer system

Khairul Kamarudin Hasan[1], Shakir Saat[2], Yusmarnita Yusop[3], Masmaria Abdul Majid[4], Mohd Sufian Ramli[5]
[1,4,5]Faculty of Electrical Engineering, Universiti Teknologi MARA (UiTM), Cawangan Johor, Kampus Pasir Gudang, Johor, Malaysia
[1,2,3]Faculty of Electronic and Computer Engineering, Universiti Teknikal Malaysia, Melaka, Malaysia
[2]School of Business and Social Sciences, Albukhary International University, Kedah Darul Aman, Malaysia

Article Info

Article history:

Received Nov 9, 2020
Revised Apr 3, 2021
Accepted Apr 23, 2021

Keywords:

Capacitive Power transfer
Class E-LCCL Inverter
Wireless Power transfer
Zero Voltage Switching

ABSTRACT

This research introduces the analysis and design of Class E-LCCL for capacitive power transfer (CPT) system. The CPT Class-E LCCL system is able to operate at high-frequency with decreased capacitance plate size and at reduced power losses by minimising switching losses. Additionally, the design of a CPT Class-E LCCL power amplifier is less complicated, since it is usually lighter and smaller with comparative intolerance to different circuit variants; hence, enabling the possibility of miniaturising the system. In this work, the capability of the CPT Class-E LCCL CPT system powered by 24 V DC supply voltage while operating at 1 MHz was analysed via experimental works and extensive simulation. Lastly, a CPT Class-E LCCL system prototype was built, generating 10 W output power via a 0.1 cm air gap at a near-perfect efficiency level of 96.68%. These findings could be beneficial for household apparatus, medical implants, and charging consumer electronics.

Corresponding Author:

Mohd Sufian Ramli
Faculty of Electrical Engineering
Universiti Teknologi MARA (UiTM)
Cawangan Johor, Kampus Pasir Gudang, Johor, Malaysia
Email: sufian6037@uitm.edu.my

1. INTRODUCTION

In this globalisation era, due to the rising popularity of wireless power transfer (WPT), the power cells of electric vehicles and mobile devices can be recharged in the absence of a charging cable or wire. The WPT shown in Figure 1 has lately received recognition as a substitution charging technique. Thus far, there exists five variants of WPT methods with non-radiation power transmission that are suitable for far-field and near-field applications: CPT, inductive power transfer (IPT), microwave power transfer (MTP), optical power transfer (OPT), and acoustic energy transfer (AET) [1]-[13]. Taking into account the weaknesses of AET's sensitivity to frequency variation and IPT's sensitivity to metal barriers [14], [15], CPT was selected in this study. CPT has the added benefits of less electromagnetic interference (EMI) and lower power loss [16], [17]. Fundamentally, CPT transmits power in a near-field application without using cables or wires but utilises an electric field instead [18]-[22]. Although IPT is a rapidly developing WPT method, it is not feasible for low power level digital devices, especially when involving compact physical spots.

Both CPT and IPT have equally excellent galvanic isolation. However, CPT is superior to IPT for high-frequency applications, as it is more cost-effective by not requiring an expensive high-frequency

magnetic core. Apart from that, CPT suitability for vehicle application was further reaffirmed when the electric field emissions were significantly decreased after using a 6-plate coupler to replace the coupling capacitive between every two plates [23]. In another study that used applied impedance matching to investigate the best operating frequency for the lowest zero voltage switching (ZVS) error, CPT was able to produce 9.5 W of output power at 95.44% efficiency with a printed circuit board plate with 2.82 nF capacitance operating at 1 MHz [24]. There are four main sections in this paper. Section II presents information about the CPT system. The analysis and design of the Class-E LCCL CPT System are presented in Section III, as well as the design specifications of the system and the experimental and simulation results, a summary of the findings is presented in Section IV.

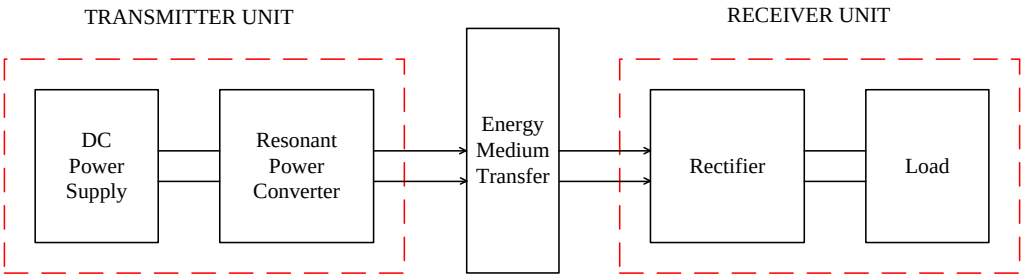

Figure 1. Simplified schematic of WPT

2. CAPACITIVE POWER TRANSFER

The CPT system utilises the electric field to transmit energy across two metal plates that behave like a capacitor. The CPT system's capacitor is linked in series to the source. Therefore, the capacitor will have an induced electric field that enables current flow to the next capacitor's section. As depicted in Figure 2, there are two general versions of the CPT structure: bipolar structure and unipolar structure. The unipolar CPT design provides power via two electric field coupling in the absence of a physical return path for the current. The directness of the unipolar CPT structure is beneficial. A study recently showed that single-wire CPT system has remarkable robustness against huge misalignment [25]. Despite being the most direct and fundamental method to create the CPT system, this design is left habitually unnoticed due to its restricted power level and grounding concerns regarding the returning conductive path. Conversely, the bipolar structure appears to be the most widespread method to create the CPT system, where 4 units of metal plates are assembled in a parallel manner to transmit power. Studies in the past confirmed the usefulness of the bipolar design for CPT; thus, it is viable to create commercial products for both high-power and low-power applications [26], [27]. Therefore, the operating principles of the bipolar structure were utilised in this work.

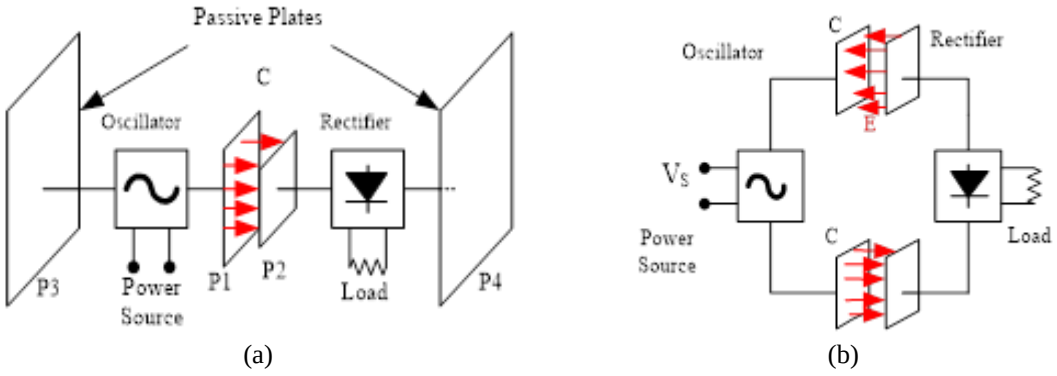

Figure 2. CPT system; (a) unipolar structure; (b) bipolar structure [28]

With the electric field coupling, the CPT method is able to overcome the limitation of the IPT method, which is the inability to transfer magnetic energy in a metallic medium. In addition, the CPT allows

transmission through metal setting, low energy loss, and excellent anti-interference in the magnetic field. The robust anti-interference trait allows the system to operate in a strong and concentrated magnetic environment; therefore, reducing energy loss [29]. Power transfer between metal obstacles is not possible in IPT since it always seeks the lowest reluctant path in the magnetic environment. Power transfer is disabled once a metal plate is placed in the middle of the power transfer system's primary and secondary coil. This is caused by eddy currents generated in the metal plates, as the magnetic field induces pole-to-pole completion along with the metal plates. This behaviour causes the IPT system to have unusably weak efficiency.

3. CPT CLASS-E LCCL CPT SYSTEM

This subsection explains the analysis and specifications of every component involved in the construction of LCCL impedance matching and Class-E resonant inverter. The Class-E MOSFET converter design focused on the switching function where the transistor is either fully ON or fully OFF. A minor overlapping in current waveforms and switch voltage will cause power loss as a result of equivalent series resistance (ESR). Losses were ignored in this work. The two main characteristics of a Class-E amplifier are: shunt capacitor installed between the switch, and a net load inductance in series to provide the essential phase shift that facilitates the fundamental wave to work as a harmonic open circuit.

The recommended Class-E LCCL CPT was observed to help to enhance the effectiveness of the overall CPT system by preserving the circumstances of ZVS to be less susceptible to broader load variants. The duty ratio or frequency can be utilised to regulate the output power, but a constant load is needed. Nevertheless, the soft switching sensitivity towards the duty ratio or frequency restricts its application, which emphasises the requirement to investigate other power electronics circuit topologies which can enhance the output power of CPT. Since the rise of output power transfer needs a greater voltage across the metal plates, it was recommended to improve the plate structure in this work while not altering the plate electric field emission or voltage. However, the system was unable to maintain high efficiency while increasing the distance between the capacitive plate. As portrayed in Figure 3, this work recommended compensation circuits for the two sides of the coupling capacitor to reduce the input impedance and magnify the output current to maximise the CPT system's power transfer limit. Essentially, the impedance matching network changes the load impedance or resistance to the required impedance to obtain a particular output power at a specific operating frequency and voltage. Figure 4 shows the circuit conversion impedance matching for Class-E LCCL CPT system.

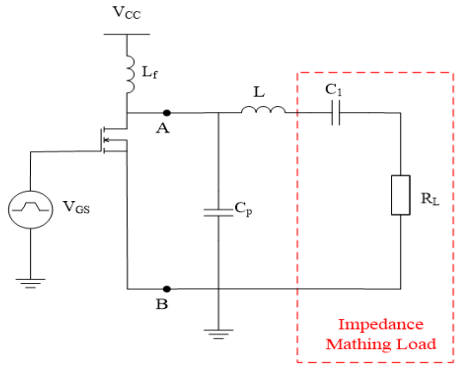

Figure 3. Basic Class-E with identify convert Impedance circuit matching

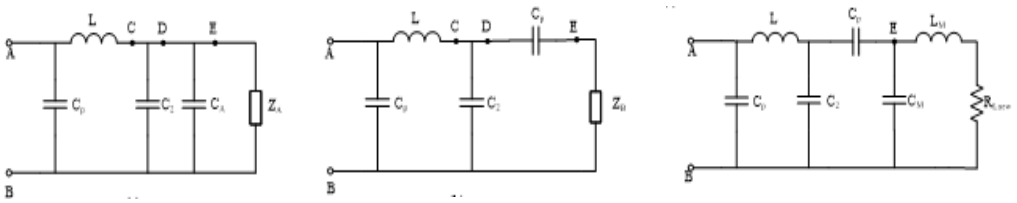

(a) (b) (c)

Figure 4. Circuit conversion impedance matching for Class-E LCCL CPT system; (a) parallel circuit Z_A-C_A; (b) series circuit Z_A-C_P; (c) parallel impedance X_{ZA}-X_c

Based on Figure 4 (b), the reactance factor of the series circuit Z_A-C_P (at the right of point D) is described as shown in (1).

$$q_D = \frac{X_{C_P}}{X_{Z_B}} = \frac{X_{Z_A}}{X_{C_A}} \quad (1)$$

The parallel circuit Z_A-C_A in Figure 4 (a) can be acquired by modifying the series circuit Z_A-C_P according to shown in (2), (3), and (4).

$$R_P = X_{Z_A}\left[\left(\frac{X_{C_P}}{X_{Z_B}}\right)^2 + 1\right] \quad (2)$$

$$X_{C_A} = X_{C_P}\left[\left(\frac{X_{Z_B}}{X_{C_P}}\right)^2 + 1\right] \quad (3)$$

$$C_P = \frac{C_P}{\frac{1}{q_d{}^2+1}} \quad (4)$$

With shown in (5), the sum of capacitance for C_A and C_2 at location C can be found.

$$\frac{1}{X_C} = \frac{1}{X_{C_A}} + \frac{1}{X_{C_2}} \quad (5)$$

The parallel impedance X_{ZA}-X_c can be transformed into the series impedance R_L-C_1 in Figure 4 by using as shown in (6), (7), and (8).

$$q_C = \frac{X_{Z_A}}{X_C} = \frac{X_{C_1}}{R_L} \quad (6)$$

$$R_L = \frac{X_{Z_A}}{1+q_C{}^2} = \frac{X_{Z_A}}{1+\left(\frac{X_{Z_A}}{X_C}\right)^2} \quad (7)$$

$$X_{C_1} = \frac{X_C}{1+\frac{1}{q_C{}^2}} = \frac{X_C}{1+\left(\frac{X_C}{X_{Z_A}}\right)^2} \quad (8)$$

As shown in (8) establishes the reactance of capacitance, while shown in (9) defines the impedance reactance factor at point C's right side:

$$X_{C_1} = \left[Q - \frac{\pi(\pi^2-4)}{16}\right]R_L \approx (Q - 1.1525)R_L \quad (9)$$

$$q_C = \frac{X_{C_1}}{R_L} = Q - 1.1525 \quad (10)$$

In contrast, the parallel impedance Z_A is conveyed in (1)1, while shown in (2) defines the impedance reactance factor at point D's right side:

$$Z_A = R_L(1 + q_c{}^2) = R_L[1 + (Q - 1.1525)^2] \quad (11)$$

$$q_D = \sqrt{\frac{X_{Z_A}}{X_{Z_B}} - 1} \quad (12)$$

By performing the calculations above, the reactance of capacitor C_P can be conveyed as shown in (14):

$$X_{C_P} = \frac{1}{\omega C_P} = q_D X_{Z_B} = X_{Z_B}\sqrt{\frac{R_L[1+(Q-1.1525)^2]}{X_{Z_B}} - 1} \quad (13)$$

$$C_P = \frac{1}{2\pi f X_{C_P}} \quad (14)$$

As shown in (15) describes the parallel reactance, whereas as shown (16) expresses the reactance X_{C2}:

$$X_C = \frac{X_{Z_A}}{q_C} = \frac{-R_L[1+(Q-1.1525)^2]}{1.1525-Q} \quad (15)$$

$$\frac{1}{X_{C_2}} = \frac{1}{X_C} - \frac{1}{X_{Z_A}} \quad (16)$$

Next, the design equation for the reactance X_{C2} is described as shown in (18), while Equation expresses C_2:

$$X_{C_2} = \frac{1}{\omega C_2} = \frac{R_L[1+(Q-1.1525)^2]}{Q-\left(\sqrt{\frac{R_L[1+(Q-1.1525)^2]}{X_{Z_B}}-1}\right)-1.1525} \quad (17)$$

$$C_2 = \frac{1}{2\pi f X_{C_2}} \quad (18)$$

In addition, the LC matching network of the series-parallel C_m-L_m transformation theorem at location E with reactance factor is defined in (19).

$$q_E = \frac{X_{L_m}}{R_{L_{new}}} = \frac{X_{Z_B}}{X_{C_m}} \quad (19)$$

As shown in (20) specifies the boosting factor (m) while as shown (21) characterises the conversion-boosting factor and resistance factor by the parallel, and the series factor of the subnetwork:

$$m = \frac{X_{Z_B}}{R_{L_{new}}} \quad (20)$$

$$q_E = \sqrt{m-1} = \sqrt{\frac{X_{Z_B}}{R_{L_{new}}} - 1} \quad (21)$$

The series reactance and L_m are defined in (3), (3), (8) and (23), respectively:

$$X_{L_m} = q_E R_{L_{new}} = \sqrt{R_{L_{new}} X_{Z_B} - \left(R_{L_{new}}\right)^2} \quad (22)$$

$$L_m = \frac{1}{2\pi f X_{L_m}} \quad (23)$$

Lastly, the parallel reactance can be formed using shown in (24), and (25) specifies C_m:

$$X_{C_m} = \frac{R_{L_{new}} X_{Z_B}}{X_{L_m}} \quad (24)$$

$$C_m = \frac{1}{2\pi f X_{C_m}} \quad (25)$$

This subsection further examines the integration of the Class-E LCCL matching network and CPT system for low-power applications utilising the single plate methodology, as shown in Figure 5. Initially, the output current, output voltage, and overall efficiency of the simulated Class-E LCCL and Class-E LC compensation designs were contrasted. Next, the study moved on to the design and construction of a 10 W Class-E LCCL CPT prototype to establish an efficient WPT through the load.

With the assumption that every condition of Class-E is greeted with a perfect switch, DC power provided by bias DC source was equivalent to the power dissipated in the load resistor. In theory, the system would achieve 100% efficiency. MATLAB simulation was done to corroborate the results of ZVS, input and output power. The capacitive coupling results at 1mm distance are tabulated in Table 1.

Figures 6 and 7 illustrates the LCCL CPT system simulation circuit and experimental setup, respectively. The closest components that match the simulation were used in the experimental work to ensure realistic results, especially when deciding the ZVS, input power, output power, and system efficiency. Results from simulation and experimental work are explained while considering a 1 mm gap across the

coupling plates. The ZVS is essential to reduce power dissipation during switching operation in MOSFET. Using ZVS, the system achieved efficient and smooth switching at V_{DS} = 87.77 V, as shown in Figure 8.

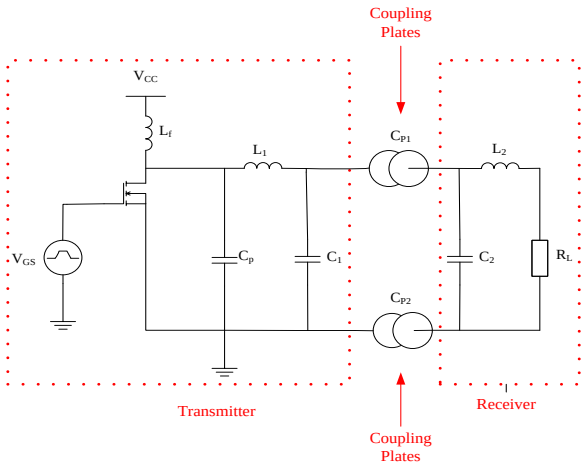

Table 1: Relevant variables.

Variable description	Variable	Note
Choke Inductor	L_1	230 µH
DC supply voltage	V_{cc}	24 V
Reactance inductor value	L_2	53 µH
Reactance capacitor value	C_1	880 pF
Transmit resonant capacitor	C_2	475 pF
Coupling capacitor value	C_P	120.9 pF
Load resistance	R_L	50 Ω
Receiver impedance Inductor	L_3	40 µH
Receiver impedance capacitor	C_3	609 pF

Figure 5. Class-E LCCL CPT system

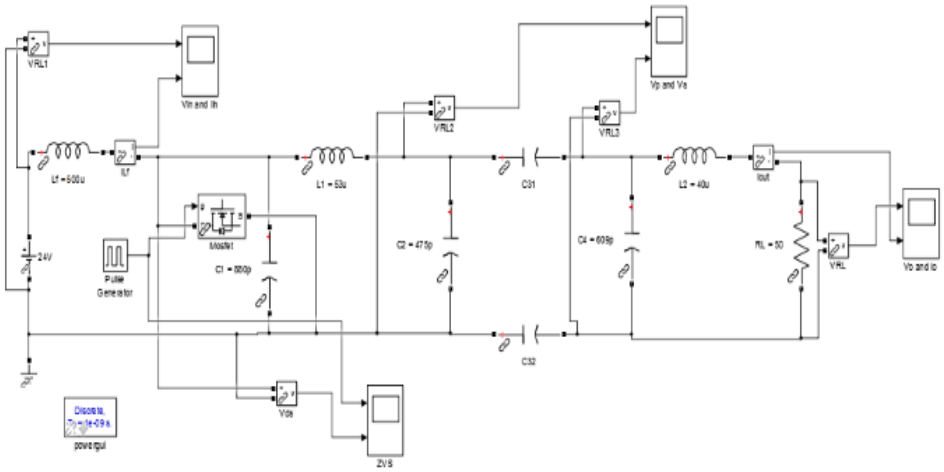

Figure 6. Schematic of the CPT LCCL system simulation in MATLAB

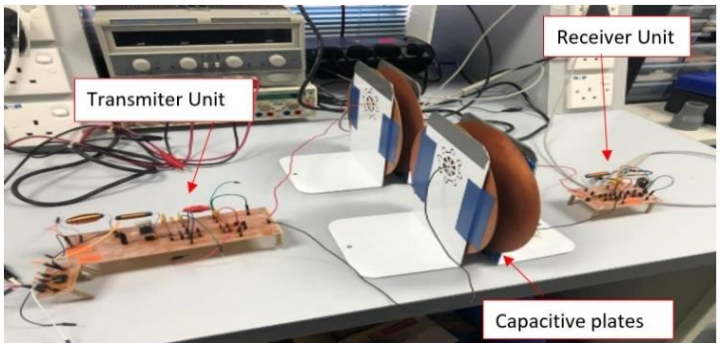

Figure 7. Experimental setup of the CPT LCCL system

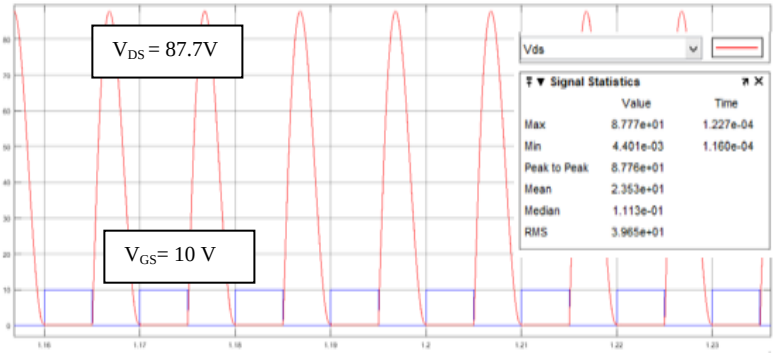

Figure 8. The ZVS simulation results of the CPT LCCL system

In the experimental work as illustrated in Figure 9, the results of ZVS were satisfactory with V_{DS} = 98 V. Both experimental and simulation results documented V_{DS} value above V_{cc} value by three to four times; indicating an outstanding value of V_{DS} switching in theory.

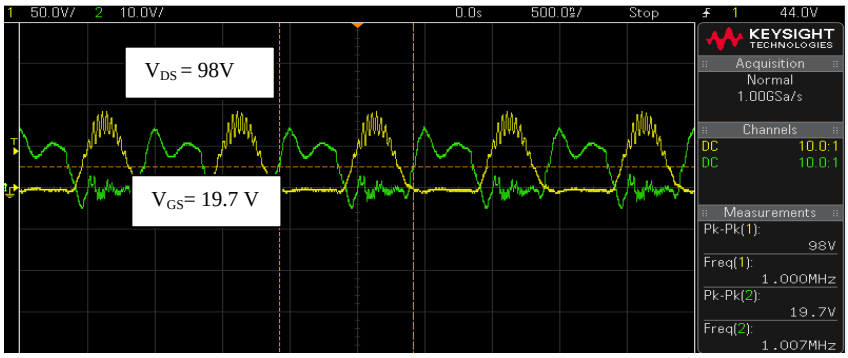

Figure 9. The ZVS experimental results of the CPT LCCL system

While reviewing the efficiency of CPT LCCL system, both input and output power simulation results are as depicted in Figure 10 and Figure 11, while the experimental results are portrayed in Figure 12 and Figure 13. The comparison between simulation and experimental work is tabulated in Table 2. Figures 10 to 13 present the power input and output outcomes; they were used to calculate the system efficiency using as shown in (26).

$$\%n = \frac{Vo(rms)*Io(rms)}{Vin(dc)*Iin(dc)} \quad (26)$$

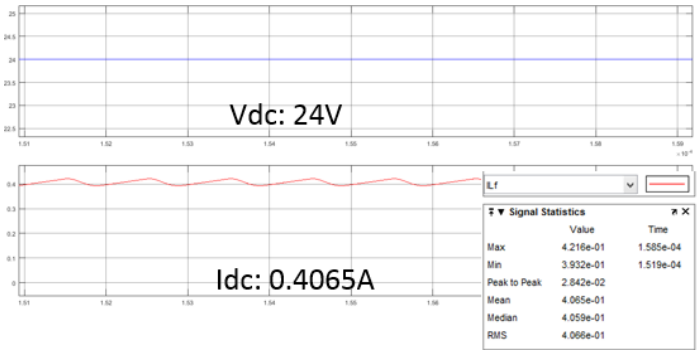

Figure 10. Current Input and voltage input simulation results

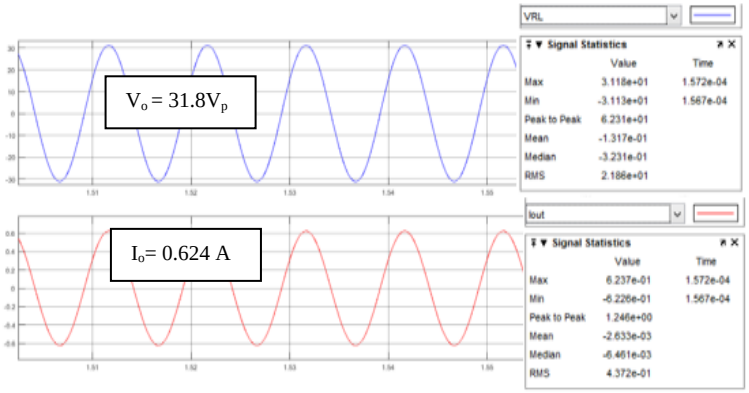

Figure 11. Current output and voltage output simulation results

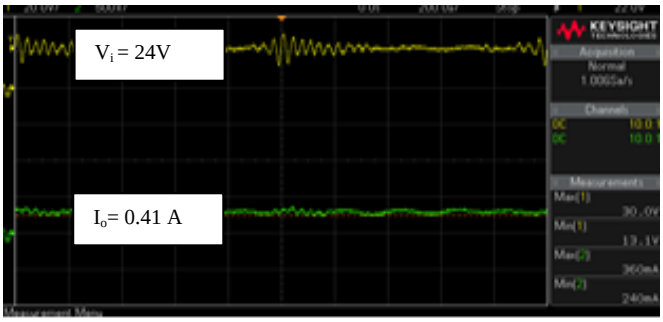

Figure 12. Current input and voltage input experimental results

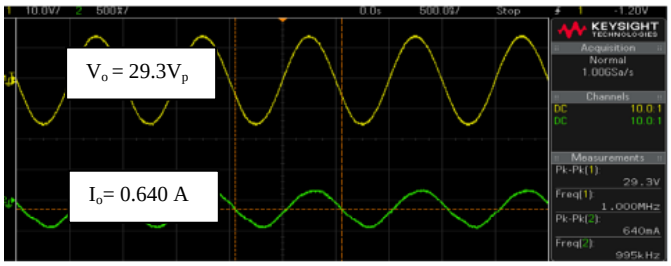

Figure 13. Current output and voltage output experimental results

Table 2 shows the efficiency of the LCCL CPT system during simulation and experiment work which are 97.96% and 96.68%, respectively. Good performance was documented for power transfer to the load at 1 mm gap across capacitance plate couplings; 10 W at 50 Ω load.

Table 2. Results of System Efficiency.

System variable	Unit Variable	Result of Simulation	Result of Experiment
Input Current (DC)	I_{in} (DC)	0.41 A	0.40 A
Input Voltage (DC)	V_{in} (DC)	24.00 V	24.10 V
Output Current (RMS)	I_o (RMS)	0.44 A	0.45 A
Output Voltage (RMS)	V_o (RMS)	21.86 V	20.71 V
Efficiency	%n	97.77%	96.68%

4. CONCLUSION

Based on the investigation outcome, power can be transferred wirelessly through the small air gap between capacitors. This work implemented a Class-E MOSFET converter in its CPT design. Consequently,

it is anticipated that WPT over a marginally lengthier gap can be improved using a number of compensation circuit designs to resonate with the capacitive coupler to generate a higher voltage, as explained in the impedance matching theory. Class-E LCCL CPT was implemented to increase the power transfer rate for a small load with low capacitive coupler variant. The experiment outcomes suggested that 9.34 W output power was achieved with 96.68% efficiency utilising the 609 pF capacitive coupling plates at 1 mm working distance. The results documented from the present investigation agrees with the findings recorded by previous literature of CPT research area. Based on the literature, high efficiency is only possible if the operating distance of the capacitive coupler is very near, usually smaller than 1 mm. Nevertheless, the performance of the entire CPT system was influenced by the power loss occurring in the rectifier and transmitter unit as well as the changes in the distance of capacitive coupling.

ACKNOWLEDGEMENTS

This research was funded by the BESTARI Research Grant Phase 3/2020 of Universiti Teknologi MARA (UiTM) Johor Branch, Malaysia [600-UiTMCJ (PJIA.5/2] grant. Sincerely to express the appreciation to Universiti Teknologi MARA (UiTM) and Universiti Teknikal Malaysia Melaka (UTeM) for professional support.

REFERENCES

[1] K. K. Hasan, Shakir Saat, Y. Yusof, M. Asraf H, Z. Mohd Yusoff, N. M. Meor Shaari, and M. Z. Mustapa, "Design of Capacitive Power Transfer (CPT) for Low Power Application using Power Converter Class E triggered by Arduino Uno Switching Pulse Width Modulation (PWM)," *Int. J. Eng. Technol.*, vol. 7, pp. 77-81, 2018, DOI: 10.14419/ijet.v7i4.22.22194.

[2] M. Meor, S. Saat, Y. Yusop, H. Husin, Z. Mustapa, and K. K. Hasan, "Design and analysis capacitive power transfer (CPT) with and without π1a impedance matching circuit for 13.56MHz operating frequency," *Proceedings-8th IEEE International Conference on Control System, Computing and Engineering, ICCSCE 2018*, 2019, pp. 99-104, DOI: 10.1109/ICCSCE.2018.8685020.

[3] C. Mi, "High power capacitive power transfer for electric vehicle charging applications," *2015 6th Int. Conf. Power Electron. Syst. Appl. Electr. Transp.-Automotive, Vessel Aircraft, PESA*, Dec. 2015, DOI: 10.1109/PESA.2015.7398937.

[4] M. Al-Saadi, L. Al-Bahrani, M. Al-Qaisi, S. Al-Chlaihawi, and A. Crăciunescu, "Capacitive power transfer for wireless batteries charging," *EEA-Electroteh. Electron. Autom.*, vol. 66, no. 4, pp. 40-51, Dec. 2018.

[5] M. A. Hannan, H. A. Hussein, S. Mutashar, S. A. Samad, and A. Hussain, "Automatic frequency controller for power amplifiers used in bio-implanted applications: Issues and challenges," *Sensors (Switzerland)*, vol. 14, no. 12. pp. 23843-23870, 2014, DOI: 10.3390/s141223843.

[6] S. Li and C. C. Mi, "Wireless power transfer for electric vehicle applications," *IEEE J. Emerg. Sel. Top. Power Electron.*, vol. 3, no. 1, pp. 4-17, Mar. 2015, DOI: 10.1109/JESTPE.2014.2319453.

[7] F. Lu, H. Zhang, T. Kan, H. Hofmann, Ying Mei, Li Cai, and Chris Mi, "A high efficiency and compact inductive power transfer system compatible with both 3.3kW and 7.7kW receivers," *Conference Proceedings-IEEE Applied Power Electronics Conference and Exposition-APEC*, 2017, pp. 3669-3673, DOI: 10.1109/APEC.2017.7931225.

[8] K. Huang and X. Zhou, "Cutting the last wires for mobile communications by microwave power transfer," *IEEE Commun. Mag.*, vol. 53, no. 6, pp. 86-93, Jun. 2015, DOI: 10.1109/MCOM.2015.7120022.

[9] T. Ishizaki and K. Nishikawa, "Wireless power beam device using microwave power transfer," *IEEE Wireless Power Transfer Conference 2014, IEEE WPTC 2014*, 2014, pp. 36-39, DOI: 10.1109/WPT.2014.6839622.

[10] S. D. Jarvis, J. Mukherjee, M. Perren, and S. J. Sweeney, "Development and characterisation of laser power converters for optical power transfer applications," *IET Optoelectron.*, vol. 8, no. 2, pp. 64-70, May 2014, DOI: 10.1049/iet-opt.2013.0066.

[11] V. F. G. Tseng, S. S. Bedair, and N. Lazarus, "Phased array focusing for acoustic wireless power transfer," *IEEE Trans. Ultrason. Ferroelectr. Freq. Control*, vol. 65, no. 1, pp. 39-49, Jan. 2018, DOI: 10.1109/TUFFC.2017.2771283.

[12] H. F. Leung, B. J. Willis, and A. P. Hu, "Wireless electric power transfer based on Acoustic Energy through conductive media," *Proceedings of the 2014 9th IEEE Conference on Industrial Electronics and Applications, ICIEA*, 2014, pp. 1555-1560, DOI: 10.1109/ICIEA.2014.6931416.

[13] H. Basaeri, D. B. Christensen, and S. Roundy, "A review of acoustic power transfer for bio-medical implants," *Smart Materials and Structures*, vol. 25, no. 12, 2016, DOI: 10.1088/0964-1726/25/12/123001.

[14] T. Zaid, S. Saat, Y. Yusop, and N. Jamal, "Contactless energy transfer using acoustic approach-A review," *I4CT 2014-1st International Conference on Computer, Communications, and Control Technology, Proceedings*, 2014, pp. 376-381, DOI: 10.1109/I4CT.2014.6914209.

[15] C. Y. Xia, C. W. Li, and J. Zhang, "Analysis of power transfer characteristic of capacitive power transfer system and inductively coupled power transfer system," *Proceedings 2011 International Conference on Mechatronic Science, Electric Engineering and Computer*, 2011, pp. 1281-1285, DOI: 10.1109/MEC.2011.6025703.

[16] K. Kh., S. Saat, Y. Yusmarnita, M. S. Ramli, and A. W. S. Sufiah, "Capacitive power transfer (CPT) system design using a class e resonant converter circuit," *AIP Conference Proceedings*, 2016, DOI: 10.1063/1.4940290.

[17] K. Kh, Shakir Saat, Y. Yusmarnita, and N. Jamal, "Analysis and Design of Wireless Power Transfer : A Capacitive Based Method for Low Power Applications," *WSEAS Trans. Circuits Syst.*, vol. 14, pp. 221-229, 2015.
[18] D. Vincent and S. S. Williamson, "Role of dielectrics in the capacitive wireless power transfer system," *Proceedings of the IEEE International Conference on Industrial Technology*, 2020, DOI: 10.1109/ICIT45562.2020.9067136.
[19] N. X. Bac, W. Peng, C. F. Hoong, X. Jianfang, and K. L. Hai, "An incorporation of DC microgrid and inductive power transfer for EV charging applications," *2017 Asian Conference on Energy, Power and Transportation Electrification, ACEPT*, 2017, pp. 1-6, DOI: 10.1109/ACEPT.2017.8168603.
[20] D. I. Oyarzun *et al.*, "Energy transfer for storage or recovery in capacitive deionization using a DC-DC converter," *J. Power Sources*, vol. 448, Feb. 2020, DOI: 10.1016/j.jpowsour.2019.227409.
[21] H. Zhang, F. Lu, H. Hofmann, W. Liu, and C. C. Mi, "Six-Plate Capacitive Coupler to Reduce Electric Field Emission in Large Air-Gap Capacitive Power Transfer," *IEEE Trans. Power Electron.*, vol. 33, no. 1, pp. 665-675, Jan. 2018, DOI: 10.1109/TPEL.2017.2662583.
[22] H. Zhang, F. Lu, H. Hofmann, and C. Mi, "An LC compensated electric field repeater for long distance capacitive power transfer," *ECCE 201-IEEE Energy Convers. Congr. Expo. Proc.*, 2016, DOI: 10.1109/ECCE.2016.7854858.
[23] H. Zhang, F. Lu, H. Hofmann, W. Liu, and C. C. Mi, "Six-plate capacitive coupler to reduce electric field emission in large air-gap capacitive power transfer," *IEEE Trans. Power Electron.*, vol. 33, no. 1, pp. 665-675, 2018, DOI: 10.1109/TPEL..2662583.
[24] Y. Yusop, S. Saat, Z. Ghani, H. Husin, and S. K. Nguang, "Capacitive power transfer with impedance matching network," *2016 IEEE 12th International Colloquium on Signal Processing & Its Applications (CSPA)*, 2016, DOI: 10.1109/CSPA.2016.7515817.
[25] L. J. Zou, A. P. Hu, and Y. G. Su, "A single-wire capacitive power transfer system with large coupling alignment tolerance," *2017 IEEE PELS Workshop on Emerging Technologies: Wireless Power Transfer, WoW*, 2017, DOI: 10.1109/WoW.2017.7959372.
[26] C. Mi, "High power capacitive power transfer for electric vehicle charging applications," *2015 6th International Conference on Power Electronics Systems and Applications (PESA)*, 2016, DOI: 10.1109/PESA.2015.7398937.
[27] H. Zhang, F. Lu, H. Hofmann, W. Liu, and C. C. Mi, "A four-plate compact capacitive coupler design and LCL-compensated topology for capacitive power transfer in electric vehicle charging application," *IEEE Trans. Power Electron.*, vol. 31, no. 12, pp. 8541-8551, Dec. 2016, DOI: 10.1109/TPEL.2016.2520963.
[28] N. Nabila, S. Saat, Y. Yusop, M. S. M Isa, and A. A. Basari, "The design of auto-tuning capacitive power transfer for rotary applications using phased-locked-loop," *International Journal of Power Electronics and Drive System (IJPEDS)*, vol. 10, no. 1, pp. 307-318, Mar. 2019, DOI: 10.11591/ijpeds.v10.i1.pp307-318.
[29] C. Xia, Y. Zhou, J. Zhang, and C. Li, "Comparison of power transfer characteristics between CPT and IPT system and mutual inductance optimization for IPT system," *J. Comput.*, vol. 7, no. 11, pp. 2734-2741, Nov. 2012, DOI: 10.4304/jcp.7.11.2734-2741.